Rare events via multiple reaction channels sampled by path replica exchange

Bolhuis, P.G.

DOI
10.1063/1.2976011
Publication date
2008

Published in
Journal of Chemical Physics

Rare events via multiple reaction channels sampled by path replica exchange

Peter G. Bolhuis[a)]
van 't Hoff Institute for Molecular Sciences, University of Amsterdam, Nieuwe Achtergracht 166, 1018WV Amsterdam, The Netherlands

(Received 9 June 2008; accepted 5 August 2008; published online 18 September 2008)

Transition path sampling (TPS) was developed for studying activated processes in complex systems with unknown reaction coordinate. Transition interface sampling (TIS) allows efficient evaluation of the rate constants. However, when the transition can occur via more than one reaction channel separated by a high barrier, TPS and TIS are ineffective in sampling both channels. The combination of replica exchange with TIS can overcome this problem. This work shows how, by including both the backward and forward reactions, the corresponding rate constants, as well as the free energy barrier can be computed in a single simulation. The method is illustrated on a two dimensional potential using the Langevin dynamics. In addition, a simpler algorithm based on only forward shooting from the interfaces is shown to give equally accurate results, and forms a bridge between the transition interface and the forward flux sampling methods. The diffusive behavior of the replicas can be used to assess the quality of the choice of the order parameter used for the interfaces. © *2008 American Institute of Physics*. [DOI: 10.1063/1.2976011]

I. INTRODUCTION

Rare events are ubiquitous in nature. The nucleation of crystals, the folding of proteins, and many chemical reactions are examples of processes that take place on time scales much longer than the molecular vibrations. This separation of time scales makes a straightforward molecular dynamics simulation very inefficient for the computation of the mechanism and kinetics of such processes. The time scale gap is caused by a high free energy barrier between the initial and final state. To overcome these high free energy barriers many computational techniques, e.g., umbrella sampling,[1] blue moon sampling,[2] metadynamics,[3] flooding,[4] local elevation, and hyperdynamics,[5] employ a biasing potential along an *a priori* defined collective variable/order parameter approximating the reaction coordinate. For the calculation of the kinetic rate constant the Bennett–Chandler procedure[6,7] corrects the transition state theory estimate based on the free energy barrier, with the so-called transmission coefficient. However, the choice of an order parameter that does not capture the reaction coordinate correctly, might result in an underestimated free energy barrier, the observation of severe hysteresis, and a statistically poor estimate of the transmission coefficient. Trajectory based simulation methods aim to alleviate this problem by focusing on the unbiased dynamic pathways connecting the initial and final states. The transition path sampling (TPS) method developed about a decade ago, performs a Monte Carlo importance sampling of trajectory space.[8,9] The basic concept of TPS is to generate a new trial trajectory from an existing valid trajectory using, for instance, the highly efficient shooting algorithm, and accept or reject that pathway according to a criterion that preserves detailed balance. The collection of paths harvested in this way provides unbiased insight into the mechanism of the reaction. Analysis of this path ensemble yields the transition state ensemble. Furthermore, by a reversible transformation of the ensemble of paths that connect the initial and final states to one that only starts the initial state, one can compute the rate constant. To perform such a transformation requires a series of path sampling simulations along (again) an order parameter, in the same spirit as umbrella sampling. However, in contrast to the bias potential based free energy methods, the TPS rate constant estimate is less sensitive to the choice of order parameter. More recently, van Erp *et al.*[10] developed the transition interface sampling (TIS) method, which improves the efficiency of the path sampling rate constant computation. This method introduces an order parameter along which a set of interfaces is constructed, and expresses the rate constant as the product of the effective positive flux through the interface close to the initial state and so-called interface crossing probabilities. For diffusive processes partial paths turned out to be sufficient, and led to the partial path transition interface sampling[11] method (PPTIS) (which is related to the Milestoning method of Faradjian and Elber[12]). Using PPTIS and TIS one can, besides the rate constant, also obtain the free energy along the order parameter directly.[13] The forward flux method by Allen *et al.*[14,15] is based on the same rate expression as TIS but is not based on the Monte Carlo importance sampling but on a sequential counting and selection algorithm. This method, originally developed to allow for nonequilibrium dynamics, also applies to equilibrium dynamics.[16]

Notwithstanding their advantages, the TPS and (PP)TIS algorithms still suffer from a few drawbacks. First, they rely on the absence of long lived intermediate states between the initial and final states. Second, due to the fact that for the shooting algorithm a new trial path resembles to a large ex-

a)Electronic mail: p.g.bolhuis@uva.nl.

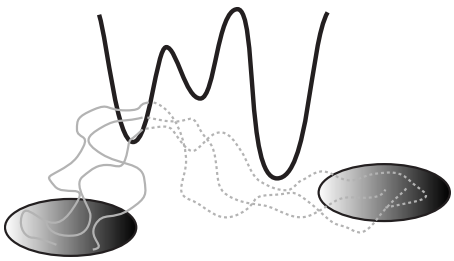

FIG. 1. The multiple channel problem. Only the left channel is sampled due to a high barrier separating it from the other channels.

tent the previous path, multiple reaction channels separated by a high barrier in between are not sampled properly (see Fig. 1). In Ref. 17 van Erp and Bolhuis proposed to resolve the latter problem by combining the TIS method with the replica exchange concept. The basic idea of this method is to perform many TIS simulations (replicas) in parallel, each at a different interface, and regularly allow for exchange between the interface ensembles, based on a detailed balance criterion. The replica exchange TIS (RETIS) method does allow for sampling multiple channels, as during a RETIS simulation a path slowly diffuses along the interfaces, and can choose another channel during this diffusion. Van Erp showed that this approach improves the efficiency of a TIS simulation substantially.[18]

The aim of the current paper is fourfold. The first aim is to extend the basic idea put forward in Ref. 17 and applied in Ref. 18 by including the backward reaction. Sampling not only the forward but also the backward pathways shows a faster convergence, yields both the forward and backward rates at once, and gives without additional effort the free energy profile. Moreover, analysis of the diffusion of the replicas in a RETIS run gives a means to asses the choice of reaction coordinates and a possible way to optimize it. The second aim is to provide insight in the advantages and limitations of the RETIS method by applying it to a simple two dimensional (2D) system. The third aim is to show the necessity of replica exchange in case of the multiple channels with unequal barrier heights. Without it, sampling is severely biased. The final aim is to introduce a variation on the RETIS theme based on forward shooting alone. This *constrained forward shooting* RETIS resembles the forward flux sampling (FFS) algorithm and can be viewed as a bridge between the FFS and TIS frameworks.

In Ref. 19 Vlugt *et al.* proposed a parallel tempering (PT), also known as replica exchange, algorithm to sample different reaction channels, by using higher temperature to overcome the barrier between the channels. Although this can be very effective for some processes, many processes, such as reactions with multiple reaction sites or diffusion through membranes, occur via reaction channels that are separated by such a high barrier that elevation of the temperature is not enough to enable switching of transition paths. Moreover, the PT version of TPS does not give the rate constants and free energy directly.

This paper is organized as follows. In Sec. II I describe the methodology using a slightly different notation compared to Refs. 17 and 18, to allow for a simple description of both the backward and forward path ensembles. This approach incorporates all path sampling methods into one framework, which I give in more detail in the Appendix. In Sec. II A the RETIS method is briefly recapitulated. The extension to the backward reaction is given in Sec. II B. Section II C introduces the novel constraint forward shooting technique. Section II D shows how to construct the free energy and the rate constant efficiently from the path sampling data. In Sec. III the RETIS method is tested on a simple 2D potential with the Langevin dynamics. The necessity of the replica exchange is illustrated in Sec. III C. The correctness of the constraint forward shooting algorithm is demonstrated in Sec. III D, followed by a discussion of the direct free energy computation. This paper ends with concluding remarks.

II. METHODS

A. Replica exchange transition interface sampling

A discretized trajectory or path $x(L)$ consists of $L+1$ times slices x_i, with $0 \leq i \leq L$. The time slices along the trajectory are separated by an interval Δt. A time slice $x=\{r,p\}$ contains all positions r and momenta p of the system. The trajectory is generated by the dynamics of interest, e.g., Hamiltonian or Langevin dynamics.

The starting point of transition interface sampling (TIS) is the division of phase space into a series of $n+1$ interfaces defined by $\lambda(x)=\lambda$, with λ being a suitable order parameter capable to distinguish final state B from initial state A. The interface $\lambda_0=\lambda_A$ is identified with the initial state, whereas the interface $\lambda_n=\lambda_B$ is identical to the boundary of B. In the following I assume that this order parameter increases monotonically, i.e., $\lambda_{i-1}<\lambda_i<\lambda_{i+1}$. The central result of TIS is the expression for the rate constant[10]

$$k_{AB} = \phi_{01} P_A(\lambda_B|\lambda_1) = \phi_{01} \prod_{i=1}^{n-1} P_A(\lambda_{i+1}|\lambda_i). \quad (1)$$

The first equality factorizes the rate in a effective positive flux ϕ_{01} through interface λ_1 and a crossing probability $P(\lambda_B|\lambda_1)$ that a trajectory coming from A and crossing the first interface reaches stable state B before reaching A.[10] The first flux factor can be computed directly in a straightforward dynamical simulation, by counting each effective positive crossing, i.e., the first crossing of interface λ_1 after having crossed λ_0. The second factor, the crossing probability $P(\lambda_B|\lambda_1)$, is more difficult to compute, but can be expressed (see the second equality) as a product of crossing probabilities over each interface λ_i. Each of the $P(\lambda_{i+1}|\lambda_i)$ crossing probabilities can be computed by performing a path sampling simulation that constrains the path to start in A, cross the interface λ_i, and end at λ_{i+1} or go back to A. This path sampling simulation comprises a Monte Carlo random walk through trajectory space, creating a new trial path from a current path and accepting or rejecting it by an appropriate Metropolis rule. The efficient shooting algorithm[20] creates a new path (n) by choosing a time slice sp (the shooting point) on the current path (o), perturbing it slightly, and shooting off a new path using the underlying dynamical equations of

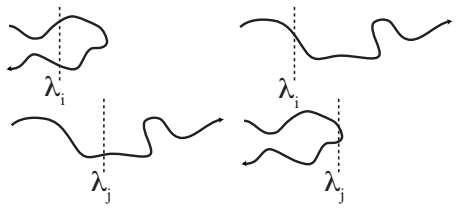

FIG. 2. The essence of the swapping of paths. On the left the current pathways of two arbitrary interface ensembles i and j are plotted. In the right these pathways are exchanged. If they belong to the other ensemble, i.e., if the paths cross the interface, as is the case in this figure, the exchange is accepted. Otherwise, the exchange is rejected.

motion. The Metropolis acceptance rule that maintains the correct path distribution is (see Appendix)

$$P_{\mathrm{acc}}[\mathbf{x}^{(o)} \to \mathbf{x}^{(n)}] = \tilde{h}_i[\mathbf{x}^{(n)}(L^{(n)})]\min\left[1, \frac{L^{(o)}+1}{L^{(n)}+1}\frac{\rho(x_{sp}^{(n)})}{\rho(x_{sp'}^{(o)})}\right], \tag{2}$$

where $\rho(x)$ denotes the steady state distribution and $\tilde{h}_i[\mathbf{x}(L)]$ is an indicator function equaling unity if the path $\mathbf{x}(L)$ belongs to the TIS ensemble i—i.e., it begins in A, crosses λ_i and goes on to λ_{i+1} or returns to A—and zero otherwise. (see Appendix and Ref. 17 for a more extended discussion).

For stochastic dynamics a change in the shooting point is not required as the random history will automatically cause a divergence.[20] In that case $\rho(x_{sp}^{(n)}) = \rho(x_{sp'}^{(o)})$ and the acceptance rule simplifies into

$$P_{\mathrm{acc}}[\mathbf{x}^{(o)} \to \mathbf{x}^{(n)}] = \tilde{h}_i[\mathbf{x}^{(n)}(L^{(n)})]\min\left[1, \frac{L^{(o)}+1}{L^{(n)}+1}\right]. \tag{3}$$

In fact, it is not necessary to limit the trajectories to the next interface λ_{i+1}. If instead the paths are allowed to go all the way to interface λ_B all interface histograms can be joined together using the weighted histogram analysis method (WHAM).[21] The corresponding indicator function $\tilde{h}_i[\mathbf{x}(L)]$ is given in Eq. (A16) of the Appendix.

Performing *time reversal* moves, in which the sequence of the time slices is inverted, and all momenta are reversed, improves the sampling. In the regular TIS method a reversal move is accepted if the path begins and ends in A, and rejected otherwise.[20] The sampling improvement stems from the fact that a reversed pathway has a different history (what was first the forward part, is now the backward part), and can thus help in decorrelating path quicker.

Although a sequential evaluation of the TIS ensembles is possible, it is efficient to perform a computation of all interfaces simultaneously in parallel. As was proposed in Ref. 17 this allows for a replica exchange approach also called path swapping. A path belonging to the λ_i interface that also crosses λ_{i+1} is a valid member of the ensemble of λ_{i+1} interface. Therefore it is possible to exchange both i and $i+1$ paths without penalty (see Fig. 2). The corresponding metropolis acceptance rule is (see Appendix)

$$P_{\mathrm{acc}}(i \leftrightarrow j) = \tilde{h}_i[\mathbf{x}^{(j)}(L^{(j)})]\tilde{h}_j[\mathbf{x}^{(i)}(L^{(i)})], \tag{4}$$

Exchanging paths between interface ensemble replicas can enhance ergodicity of the path ensemble substantially.[18]

Paths in the TIS ensemble belonging to the first and last interface are rather short, and do only change slowly during sampling. Using the additional ensembles for the first and last interface proposed by van Erp in Ref. 18 one can explore different parts of the λ_1 interface, thus tremendously increasing the exploration efficiency. A path in the additional ensemble for the first interface starts at the first interface and explores the stable state A, until it crosses the first interface again. For the last interface λ_{n-1} a similar definition of an additional ensemble holds. Note that the interfaces λ_0 and λ_n do not have a ensemble connected to it, but are simply the stable state boundaries.

B. Including the backward reaction

Because in the replica exchange TIS all interface ensembles are sampled simultaneously the calculation of the reverse process B to A is easily included. For that the indicator function should not only allow for AA and AB paths but also include BA and BB paths. Defining adjacent phase space regions separated by interface λ_i as $\Lambda_i^+ = \{x : \lambda(x) > \lambda_i\}$ and $\Lambda_i^- = \{x : \lambda(x) < \lambda_i\}$ the indicator function for this path ensemble becomes

$$\breve{h}_i[\mathbf{x}(L)] = \begin{cases} 1 & \text{if } x_0 \in (A \cup B) \wedge x_L \in (A \cup B) \wedge \\ & \forall\{j | 1 < j < L\} : x_j \notin (A \cup B) \wedge \\ & \exists\{j | 1 < j < L\} : x_j \in \Lambda_i^- \wedge \\ & \exists\{j | 1 < j < L\} : x_j \in \Lambda_i^+ \\ 0 & \text{otherwise.} \end{cases} \tag{5}$$

The indicator function $\breve{h}_i[\mathbf{x}(L)]$ selects paths that lead from A crossing the λ_i interface and reach A or B, or lead from B crossing the λ_i interface and reach A or B. The acceptance rule is given as in Eq. (3)

$$P_{\mathrm{acc}}[\mathbf{x}^{(o)} \to \mathbf{x}^{(n)}] = \breve{h}_i[\mathbf{x}^{(n)}(L^{(n)})]\min\left[1, \frac{L^{(o)}+1}{L^{(n)}+1}\right]. \tag{6}$$

The replica exchange swap acceptance for this ensemble is given by

$$P_{\mathrm{acc}}(i \leftrightarrow j) = \breve{h}_i[\mathbf{x}^{(j)}(L)]\breve{h}_j[\mathbf{x}^{(i)}(L)]. \tag{7}$$

In RETIS, it is convenient to choose $\lambda_0 = \lambda_1$ and $\lambda_n = \lambda_{n-1}$. The exchange between the first interface ensemble and its additional ensemble is then simply done by extending the path of the additional ensemble in the forward direction until it recrosses the interface λ_0, and extending the path of the first interface ensemble in the backward direction until it recrosses the interface λ_0. For both paths, the old trajectory part is completely deleted, except for the two slices just before and after crossing the λ_0 interface. This swap move can always be accepted, as the paths in both the additional and the normal TIS ensemble always will cross their interface (see Ref. 18). The exchange between the last interface ensemble and its additional ensemble is done similarly.

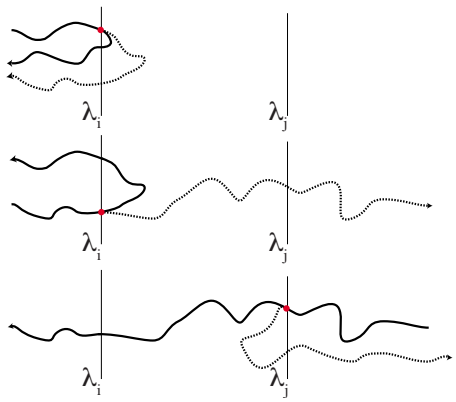

FIG. 3. (Color online) A possible sequence of events in constrained forward shooting. In the top situation the solid current *AA* path has its first crossing point with interface *i*, indicated by the circle. A forward shot from the shooting point always ends in a valid path. In the middle situation a time reversal has taken place, and from the new shooting point the final state is reached. This *AB* path is in the bottom situation exchanged with that of interface *j* (hence the new shooting point) and time reversed. A new forward shot leads now to a *BB* path.

C. Constrained interface shooting

While by definition RETIS has higher shooting acceptance ratio than regular TIS, because all possible paths (*AA*, *AB*, *BA*, and *BB*) are included in the ensemble, the acceptance ratio can be further improved by applying a biasing function as is discussed in the Appendix. In fact, the acceptance ratio can become even higher by only selecting shooting points at the interface, because then all paths will cross the interface at least once by definition. The acceptance ratio depends only on the number of interface crossings C_i.

$$P_{\mathrm{acc}}[\mathbf{x}^{(o)} \to \mathbf{x}^{(n)}] = \breve{h}_i(\mathbf{x}^{(n)}(L^n))\min\left[1, \frac{C_i^{(o)}}{C_i^{(n)}}\right]. \tag{8}$$

The number of recrossings might change rapidly from one path to the next, reducing the acceptance ratio again. However, if one always selects the first crossing point as a shooting point, the acceptance will only depend on the indicator function

$$P_{\mathrm{acc}}[\mathbf{x}^{(o)} \to \mathbf{x}^{(n)}] = \breve{h}(x^{(n)}(L^n)). \tag{9}$$

At first sight, no proper sampling seems possible as the shooting point does not change. However, the time reversal move will provide a new first crossing point thus allowing for proper sampling (see Fig. 3). Moreover, now both the shooting and the reversal move acceptance ratio are 100%. This approach requires only shooting in the forward direction at the first shooting point, as shooting backward might change the location of the first shooting point, and hence destroy detailed balance. Therefore, this implementation currently can only be used for stochastic dynamics.

While the improvement of acceptance seems substantial, it remains to be seen whether it does improve the accuracy of the sampling, as the decorrelation of the paths might be slower than for the regular RETIS implementation with variable shooting point. However, the constrained shooting RETIS has the advantage of a simpler algorithm, and the advantage of a smaller memory storage. The latter point follows from the fact that only the interface crossing point time slices are needed. For simulation techniques that require a large storage, such as Car-Parrinello molecular dynamics (CPMD), this can be a major issue.

Note that this implementation of RETIS has a great resemblance to FFS, as the paths are always shot from the interface and in the forward direction. In fact, this implementation of the TIS methods is a clear link to the FFS methods.[14,15] The constrained forward shooting RETIS, in fact, allows relaxation of FFS trajectories, with a minimum of additional computational effort.

D. Rate constant and free energy

The interface ensembles yield the crossing probability histograms as well as the population histograms as a function of λ, and hence the free energy. The crossing probability histograms can be extracted from the sampling results by separating the *AA* and *AB* paths from the *BB* and *BA* paths from each ensemble λ_i. The crossing probability for the final state is then simply given by the number of *AB* paths over the total number of paths in the ensemble $P_A(\lambda_B|\lambda_i) = \#AB/(\#AA+\#AB)$. As in the regular TIS approach the crossing probability histograms $P_A(\lambda|\lambda_i)$ can be extracted from the *AA* and *AB* paths by

$$P_A(\lambda|\lambda_i) = \langle \theta(\lambda_{\max}[\mathbf{x}(L)] - \lambda) h_A(x_0) \rangle_{\lambda_i}, \tag{10}$$

$$\equiv \int \mathcal{D}[\mathbf{x}] \mathcal{P}_i[\mathbf{x}(L)] \theta(\lambda_{\max}[\mathbf{x}(L)] - \lambda) h_A(x_0), \tag{11}$$

where $\lambda_{\max}[\mathbf{x}(L)]$ is the maximum value of λ reached on the path $\mathbf{x}$, and $\theta(x)$ is the Heaviside step function. The subscript λ_i in the average denotes that all paths need to cross λ_i. The $h_A(x_0)$ function ensures that only paths starting in *A* are being selected. The path integral in the second line runs over all possible paths of all lengths. The path probability $\mathcal{P}_i[\mathbf{x}(L)$ is defined in Eq. (A24) of the Appendix. Similarly the backward crossing probability is

$$P_B(\lambda|\lambda_i) = \langle \theta(\lambda - \lambda_{\min}[\mathbf{x}(L)]) h_B(x_0) \rangle_{\lambda_i}, \tag{12}$$

where $\lambda_{\min}[\mathbf{x}(L)]$ is now defined as the minimum value of λ reached on the path $\mathbf{x}$ and the $h_B(x_0)$ function ensures that only paths starting in *B* are being selected.

Joining these crossing probability histograms with WHAM (Ref. 21) yields $P_A(\lambda|\lambda_1)$ and $P_B(\lambda|\lambda_{n-1})$. The forward and backward rate constants follow from $k_{AB} = \phi_{01} P_A(\lambda_B|\lambda_1)$ [Eq. (1)] and its backward version $k_{BA} = \phi_{n,n-1} P_B(\lambda_A|\lambda_{n-1})$, respectively. The flux factors ϕ_{01} and $\phi_{n,n-1}$ are, respectively, given by the number of effective positive crossings of a long trajectory initiated in *A* with the first interface and that of a trajectory initiated in *B* with the last interface $n-1$, divided by the total time of the trajectory.[10,22] In the replica exchange TIS the introduction of the additional ensembles immediately give the flux factor.[18] The sum of the average trajectory length (in time) of the additional ensemble τ^- and that of the first interface τ_1 is then equal to the inverse of the flux: $\phi_{01}^{-1} = \langle \tau^- + \tau_1 \rangle$. A similar definition hold for the flux of the reverse reaction.

Not only the rate constants can be extracted but also the free energy profiles along the λ parameter. From long unconstrained trajectories of length L this would follow immediately by taking the logarithm of the histogram to find the trajectory at λ

$$F(\lambda) = -k_B T \ln p(\lambda) + \text{const}, \tag{13}$$

where k_B is Boltzmann's constant, and

$$p(\lambda) = \left\langle \sum_{k=0}^{L} \delta(\lambda(x_k) - \lambda) \right\rangle, \tag{14}$$

where $\delta(x)$ is the Dirac delta function.

For the constrained trajectories of the path ensemble the situation is slightly different. Just applying the above recipe leads to a bias because many trajectories are excluded from the ensemble due to the crossing constraint. However, for two interfaces λ_i and $\lambda_j > \lambda_i$, the ensemble of trajectories from A that cross λ_i combined with the trajectories from B that cross λ_j in the reverse direction, constitute *all* possible pathways between λ_i and λ_j. It is useful to define the conditional distributions for each interface

$$p_{Ai}(\lambda) = \left\langle \sum_{k=0}^{L} \delta(\lambda(x_k) - \lambda) h_A(x_0) \right\rangle_{\lambda_i} \quad \text{for } \lambda > \lambda_i, \tag{15}$$

which gives the probability to be at a value of λ while on a path coming from A and crossing λ_i. Similarly for paths coming from B and crossing j one can define

$$p_{Bi}(\lambda) = \left\langle \sum_{k=0}^{L} \delta(\lambda(x_k) - \lambda) h_B(x_0) \right\rangle_{\lambda_j} \quad \text{for } \lambda < \lambda_j, \tag{16}$$

The total probabilities $p_A(\lambda)$ and $p_B(\lambda)$ are given by

$$p_A(\lambda) = \sum_{i=0}^{n} s_{Ai} p_{Ai}(\lambda), \tag{17}$$

$$p_B(\lambda) = \sum_{i=0}^{n} s_{Ai} p_{Bi}(\lambda), \tag{18}$$

where the scaling factors s_{Ai} and s_{Bi} follow from WHAM.[21] In principle, these distributions can be obtained from two regular TIS simulations, whether or not using replica exchange. The total probability $p(\lambda)$ is simply obtained by matching the two histograms at a certain interface i.

$$p(\lambda) \propto s_{AB}(\lambda_i) \frac{p_A(\lambda)}{p_A(\lambda_i)} + s_{BA}(\lambda_i) \frac{p_B(\lambda)}{p_B(\lambda_i)}. \tag{19}$$

The scaling factor $s_{AB} = m_{Ai}(\lambda_i)/m_{AB,i}(\lambda_i)$ where $m_{Ai}(\lambda_i)$ is the unnormalized and unmatched p_{Ai} histogram for the region λ_i to λ_{i+1}, and $m_{AB,i}(\lambda_i)$ is the unnormalized and unmatched histogram for the AB paths only for the same region. Similarly, $s_{BA} = m_{Bi}(\lambda_i)/m_{BA,i}(\lambda_i)$, with $m_{Bi}(\lambda_i)$ the unnormalized and unmatched p_{Bi} histogram for the region λ_{i-1} to λ_i, and $m_{AB,i}(\lambda_i)$ the BA histograms for the same region. In short, this rescaling matches the AB histograms with the BA histograms for each region, as they should be exactly the same by definition. (The BA and AB histograms were called the boundary histograms in Ref. 13).

If the rates are known, an alternative way to add the histograms $p_A(\lambda)$ and $p_B(\lambda)$, follows from the detailed balance condition $p_A k_{AB} = p_B k_{BA}$ or,

$$\frac{\int_A d\lambda p(\lambda)}{\int_B d\lambda p(\lambda)} = \frac{k_{BA}}{k_{AB}}, \tag{20}$$

where the integrals run over the stable state regions A and B. Realizing that Eq. (19) actually involves only a single relative weight factor c

$$p(\lambda) \propto p_A(\lambda) + c p_B(\lambda), \tag{21}$$

it follows that

$$\frac{\int_A d\lambda (p_A(\lambda) + c\int_A d\lambda p_B(\lambda))}{\int_B d\lambda p_A(\lambda) + c\int_B d\lambda p_B(\lambda)} = \frac{k_{BA}}{k_{AB}}. \tag{22}$$

Solving c gives the full histogram, and the correct free energy. A similar histogram analysis has been proposed in Ref. 16 for the FFS technique.

III. RESULTS AND DISCUSSION

A. Model

In this section I show the necessity of replica exchange for correct sampling of multiple routes by applying RETIS to simple $2d$ potentials using the Langevin dynamics (LD). All LD simulation are done using the algorithm detailed in Ref.

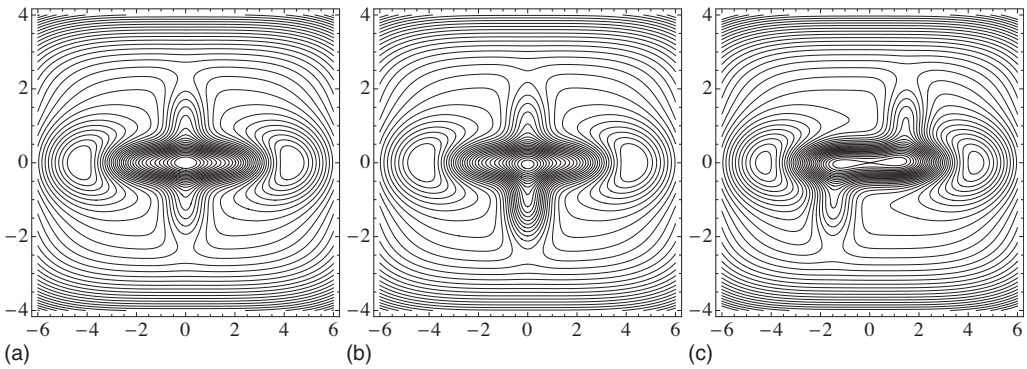

FIG. 4. The 2D model potential used for the calculations in the paper. There are two minima connected via two channels. (a) The barriers are at the same location and at the same height. (b) The lower barrier is higher then the upper barrier. (c) The barriers are of equal height, but placed asymmetrically along the x axis.

8, with a time step $\Delta t=0.05$ and a friction of $\gamma=2.5$. The inverse temperature $\beta=1/k_BT$ determines the effective rate constant. Here, T is the reduced (artificial) temperature and k_B is the Boltzmann constant.

The simple $2d$ model potential consists of a two state system that is connected by two routes.[23] The mathematical form of the potential is given by

$$V(x,y) = -3e^{-0.25(x-4)^4-y*y} - 3e^{-0.25(x+4)^2-y^2} + \frac{32}{1800}(0.0625x^4+y^4) + 5e^{-(0.0081x^4+4y^2)} + 2e^{-1.5(x-b)^2-(y-1)^2} + 2ae^{-1.5(x+b)x^2-(y+1)^2}. \quad (23)$$

Two possible routes exist between the two minima, separated by a large barrier. By changing b the relative position of the barriers shifts along the x axis. The variable a changes the height of one of the barriers. The RETIS method will be applied to three different situations corresponding to different values of a and b. These three instances of the potential are shown in Fig. 4. In all three situations the two minima are located at $(x,y)=(-4.30,0)$ and $(x,y)=(4.30,0)$. The first situation corresponds to the values $a=1,b=0$ and shows a symmetric potential with barriers of equal height $V=3.1$ located at $x=0,y=-2.33$ and $x=0,y=2.33$. The second case is a symmetric potential in which the barriers are of unequal height: $a=2,b=0$. The upper one with a height $V=3.10$ is located at $x=0,y=2.33$, the lower one with a height $V=3.35$ is located at $x=0,y=-2.53$. The height difference between the two barriers is only $\Delta V=0.25$ but will be of importance for low temperatures. The third example is $a=1,b=1.5$, an asymmetric potential in which the two barriers have the same height $V=3.11$ but are shifted along the x axis. They are located at, respectively, $x=-1.51,y=-2.33$ and $x=1.51,y=2.33$.

B. Rate calculation

The reference values for the rate constants were computed by straightforward LD at the inverse temperatures $\beta=2,3,4$, for each of the potentials. The total simulation time was $t=2.5\times10^7$. For all potentials the forward rate is equal to the backward rate due to symmetry. Hence the rate is simply the number of A to B crossings per unit time. The order parameter $\lambda\equiv x$, separates the states sufficiently. Note that while the 2D model is simple, it does describe a realistic situation where one knows the order parameter that distinguishes the states (x), but the location of the barriers and the number of channels is unknown. In all simulations region A is defined as $\lambda<\lambda_0=-3.7$ and B as $\lambda>\lambda_n=3.7$. The results are given in Tables I–III.

TABLE I. Rate constants for symmetric potential with equal barrier heights $(a=1,b=0)$ for different temperatures. The subscript denotes the error in the last digit(s) based on a block average.

	$\beta=2$	$\beta=3$	$\beta=4$
LD rate	$2.97_5\times10^{-4}$	$1.59_5\times10^{-5}$	$7_4\times10^{-7}$
TIS flux	0.067_5	0.036_2	0.020_1
TIS cross probability	0.0045_1	0.00040_2	$3.6_2\times10^{-5}$
TIS rate	0.00030_1	$1.47_7\times10^{-5}$	$7.4_5\times10^{-7}$
Ratio	1.02	0.92	1.0

TABLE II. Rate constants for symmetric potential with uneven barrier heights $(a=2,b=0)$ for different temperatures.

	$\beta=2$	$\beta=3$	$\beta=4$
LD rate	$2.25_2\times10^{-4}$	$1.11_4\times10^{-5}$	$4.6_{12}\times10^{-7}$
TIS flux	0.067_5	0.036_2	0.020_1
TIS cross probability	3.4_110^{-3}	2.9_210^{-4}	2.4_210^{-5}
TIS rate	2.27_710^{-4}	1.07_810^{-5}	4.9_510^{-7}
Ratio	1.01	0.97	1.04

Next, the rate constants were calculated using replica exchange TIS for the same temperature range. Twenty seven interface replicas were initiated at $x=-3.7$, -3.55, -3.4, -3.2, -2.9, -2.6, -2.2, -1.8, -1.5, -1.2, -1.0, -0.8, -0.5, 0, 0.5, 0.8, 1.0, 1.2, 1.5, 1.8, 2.2, 2.6, 2.9, 3.2, 3.4, 3.55, and 3.7. Two additional replicas for the first and last interfaces were introduced, in accordance with the strategy proposed by van Erp to increase efficiency and compute the flux within the TIS simulation itself.[18] For the production run the number of cycles was 10 000, the number of shots per cycle per replica was 10, the number of time reversals 10 per cycle per replica, and the number of attempted replica exchange was 200 per cycle. The average shooting acceptance ratio is about 60%–80%. The time reversal acceptance is of course 100% as all possible pathways are allowed. The exchange acceptance varies between 30% and 60%. While the flux factor is given by the average path lengths in additional ensembles, the flux factor is also measured independently for interface $x=3.55$. The crossing probabilities are histogrammed for the forward and reverse barrier transitions AB an BA, and the final crossing probability is obtained using WHAM. Combining the crossing probability with the flux yields the rates, also given in Tables I–III. The difference between the RETIS rates and the straightforward LD is within the estimated error bar of less than 10%, indicating that the RETIS method indeed gives the correct results (Fig. 5). This is not surprising considering that regular TIS gives correct rates for a simple $2d$ potential. As was shown in Ref. 18, RETIS is much more efficient than straightforward TIS. The rate computed with the flux estimate from the first ensemble is also consistent with the rate computed based on the $\lambda=3.55$ interface.

C. Assessing the sampling of multiple channels using replica exchange

Not surprisingly, for the symmetric and the asymmetric potential with equal barrier height both routes are sampled

TABLE III. Rate constants for the asymmetric potential with equal barrier heights $(a=1,b=1.5)$ for different temperatures.

	$\beta=2$	$\beta=3$	$\beta=4$
LD rate	$3.01_1\times10^{-4}$	$1.62_4\times10^{-5}$	$7.6_{12}\times10^{-7}$
TIS flux	0.067_5	0.036_2	0.020_1
TIS cross probability	5.0_410^{-3}	4.3_510^{-4}	3.5_410^{-5}
TIS rate	3.4_310^{-4}	1.6_210^{-5}	7.2_910^{-7}
Ratio	1.12	0.97	0.95

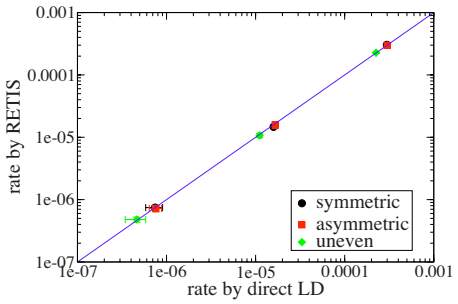

FIG. 5. (Color online) The RETIS rates compared to the straightforward simulation results (cf. Tables I–III).

with equal frequency. At first sight it seems that performing a TIS simulation without the replica exchange, would reduce the rate by a factor of 2 because, in that case, only one channel is sampled. However, it turns out that the rates are unchanged with respect to RETIS and regular LD. Hence, a TIS estimate of only one of the barriers will give a good indication of the rate. This is caused by the fact that the crossing probabilities are independent of which channel has been taken. The simulations show that for some replicas in the initial part of the barrier switching between the routes still occur. At a certain point the barrier between the routes is too high to allow for switches. From that moment on all the flux is channeled through one route. Because the TIS method assumes that the sampling of the ensembles on the interfaces is correct, the crossing probability is continuous even if most of the path ways in the "wrong" channel are going nowhere. TIS, by staying in one channel, makes an error but arrives at the correct answer because the barriers are equally high.

Next, I will show that for a system that has multiple transition routes with different barrier heights replica exchange TIS is mandatory to sample properly. For a symmetric uneven barrier one can set $a=2, b=0$. Note that setting $a=2$ does not imply that the barrier is twice at high. Instead the barrier is only $\Delta V=0.25$ higher. For the TIS simulation the initial path is led through the higher barrier, because this will show the largest difference with the RETIS (restricting the TIS sampling to the slightly lower barrier, will naturally show a smaller difference as the higher barrier has a smaller contribution to the rate). The resulting relative rate constants are plotted in Fig. 6. From this figure is clear that initializing TIS in the high barrier route one can easily make a 50%

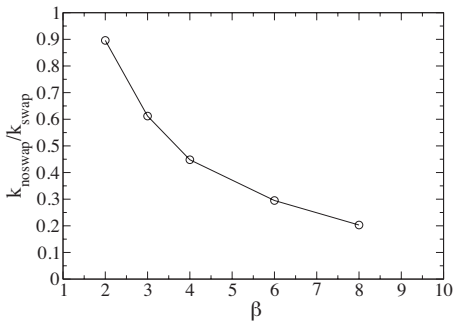

FIG. 6. The ratio of the rate constant without and with the swap move as a function of temperature. The influence of the swap move on the final predicted rate constant is substantial.

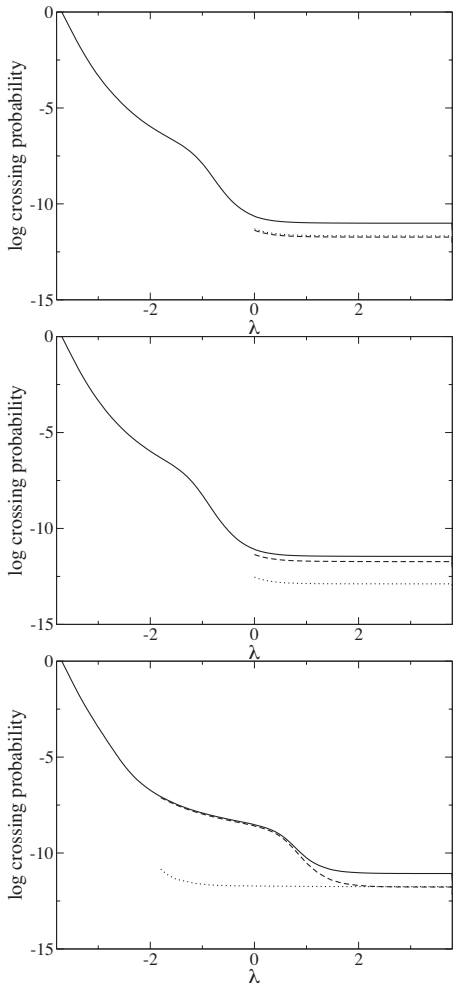

FIG. 7. The crossing probabilities $P_A(\lambda|\lambda_1)$ for the three potentials. Solid curve: The total crossing probability. Dashed curve: The crossing probability of the top channel. Dotted curve: The crossing probability of the lower channel. Top panel: Symmetric potential, middle panel: Uneven potential, lower panel: Asymmetric potential. In the case of the asymmetric potential the paths can be distinguished already from $\lambda=-1$, whereas for the other potentials only from $\lambda=0$. The sum of both partial crossing probabilities equals the total (solid curve).

error, as the lower barrier is missed. Note that I did not restrict the paths to stay in the higher barrier. The fact that it is missed is purely a sampling problem caused by the high barrier in between the routes. For lower temperatures the discrepancy becomes worse, because the difference in energy becomes more relevant. Including the replica exchange improves the situation dramatically as now both channels are sampled.

It is interesting to investigate what the different contributions of both barriers are. In principle, one can count the flux of paths through each channel. Adding the two fluxes through the two channels will give the total flux and hence the total rate. However, at the initial stage of the barrier the two routes cannot be distinguished as pathways can easily switch. Nevertheless, the two routes can easily be distinguished when they are passing the transition state at $x=0$. Counting the paths for each route trough the transition state interface gives the flux contribution for each route. The contributions to the flux from A to B are plotted in Fig. 7. For the symmetric potential with equal barriers both contributions

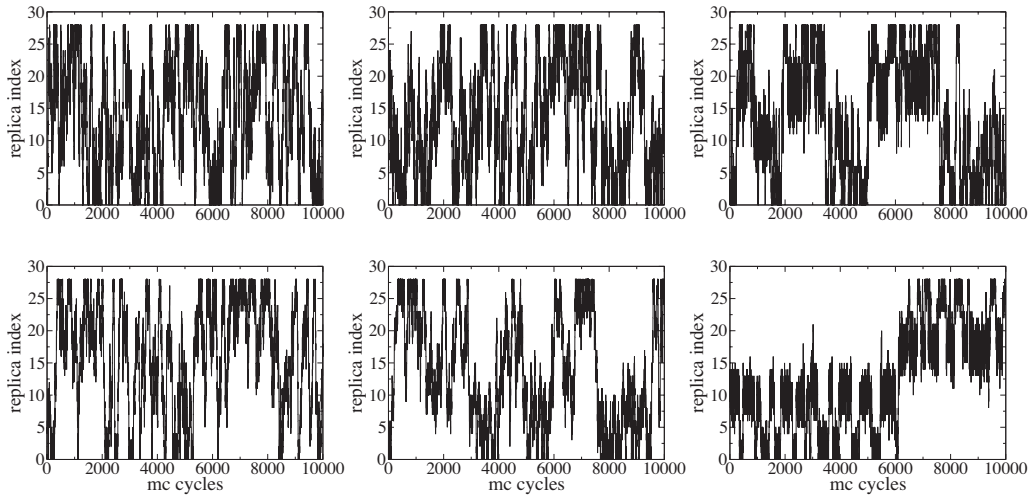

FIG. 8. The diffusion through the interface space for a single replica in the ensemble. Top row: Temperature $\beta=4$. Bottom row: Temperature $\beta=6$. Left: Symmetric even potential. Middle: Symmetric uneven, Right: Asymmetric even potential.

are the same, as is clear from the figure's top panel. For the uneven symmetric barrier, however, the lower route is much more likely than the top one. In the case of the asymmetric potential, the routes can be distinguished already when the barrier in the lower route is passed (at about $\lambda=-1.5$). Hence in the lower panel of Fig. 7, the two contributions are very different for $x=-2$, as only a small number of path will pass the lower route at that point. However, later in the barrier crossing the upper barrier needs to be passed, and eventually the two contributions join up again and the final contributions to the rate are equal.

As discussed above including replica exchange quickly allows for the exploration of both channels without much computational cost. The effectiveness of RE can be tested through an evaluation of the diffusion of replicas through interface space. The important is that the replicas all diffuse from the first to last interface and back because then the paths can switch to a different channel. The amount of diffusion through different channels is clear from Fig. 8 where the interface index of a single replica is plotted as a function of simulation time for two temperatures for the three potentials. For the symmetric even and uneven potentials at a temperature $\beta=4$ the diffusion is good and the replica visits the initial interface as well as the final interfaces many times. The turnover time is about 300 cycles for both potentials. For the lower temperature $\beta=6$ the diffusion becomes slower, with turnover time of 600 cycles.

The situation is different for the asymmetric potential, also shown in Fig. 8. At a temperature of $\beta=4$ there are still around ten turnovers, but for the lower temperature of $\beta=6$ there is on average only a single turnover. This is caused by the asymmetry of the barrier. At the positions of the barrier $(x=-2)$ and $(x=2)$ most paths are going through the other route where the barrier has not been reached yet. Only a small fraction of paths will pass the barrier at those points, but these are needed to make a successful swap between a path committed to B, and a path committed to A. The slow diffusion of replicas can be used to assess the choice of order parameter for the interfaces. Clearly, in this case the order parameter choice can be improved, such that the barriers are not at different locations as a function of λ. e.g., in this particular case $\lambda=x-y$. This optimization procedure will be addressed in a future study.

D. Constrained forward shooting

The constrained forward shooting algorithm has been tested on the symmetric potential for $\beta=4$ and gives within the error bar the same rate as RETIS. The error bars for the constrained shooting and the RETIS using the same amount of swaps, reversals, and shots per cycle are comparable. For the constrained shooting algorithm the acceptance is indeed 100%, as all new paths are shot from the first crossing point at the interface. The efficiency gain is not very large, as the shooting acceptance in the regular TIS is also very high, around 70%. This should indicate a gain of 30% but the decorrelation between paths is slightly slower, as there is a substantial chance of restarting the shot at the same shooting point as in the previous step, namely, (1) if there has been no swap or reversal accepted, (2) if there has been a doubly accepted swap or reversal. This problem does not occur in the regular RETIS version, where the shooting point is chosen randomly. Nevertheless, the resulting rate constants are as accurate for the same number of shots, and so the constrained forward shooting version is a viable alternative to the regular RETIS. The constrained shooting does show a slightly higher number of turnovers, i.e., diffusion of replicas all the way from A to B and back. This might indicate a more effective sampling.

E. Free energy calculation

The free energy can be computed from the RETIS simulation via Eq. (19). This requires matching of the separate histograms $p_{Ai}(\lambda)$ and $p_{Bi}(\lambda)$ (Eqs. (15) and (16) into respectively, $p_A(\lambda)$ and $p_B(\lambda)$ [Eqs. (17) and (18)]) and then perform the final matching in Eq. (19). As explained in Sec. II the histograms i are constructed from the parts of the paths that have crossed the interface i, as these are unbiased, i.e., all relevant pathways are in the ensemble. This is done by simply separating the AB and AA paths from the BA and BB

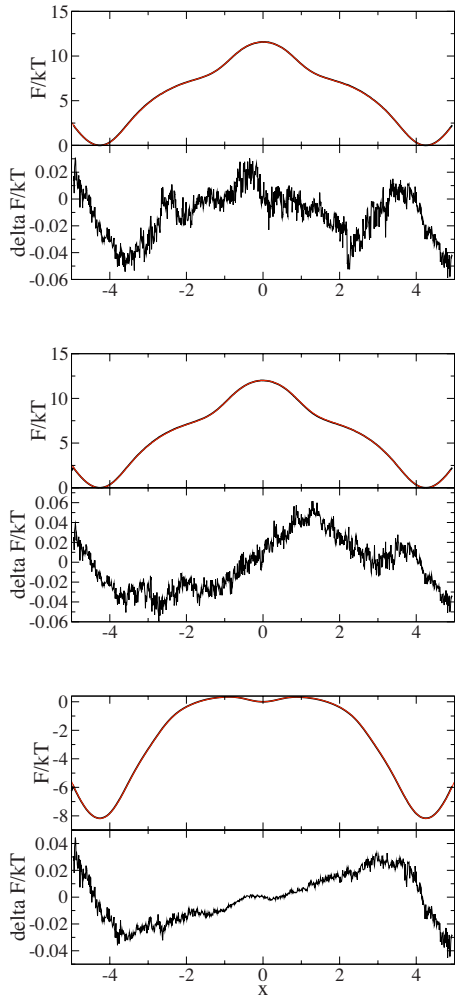

FIG. 9. (Color online) Free energy profile along $\lambda=x$ directly computed from the RETIS simulation. The lower panel shows the difference between the exact and the computed free energy.

paths in the RETIS simulation. The relative weight s_{AB} and s_{BA} of both histograms is given by the boundary histograms AB and BA.[13] In principle, one can match at any arbitrary interface using the boundary histograms, but for this case the most logical place to match is on the top of the barrier, where $s_{AB}=s_{BA}$ because of symmetry reasons.

The free energy is given in Fig. 9 and approximates the exact free energy within an error of $0.05k_BT$, corresponding to a relative error of 0.5%. The free energy barriers for the symmetric and uneven potential are very similar. The asymmetric potential shows an intermediate minimum, which is clearly caused by projecting on a order parameter which is not fit for describing the two channels.

IV. CONCLUSION

In this paper I have shown the necessity of the RETIS method for path sampling of multiple channels separated by a large free energy barrier. Moreover, the RETIS method can dramatically improve the efficiency of path sampling.[18] In addition, RETIS yields the rate constants of the forward and backward rate constants and gives the correct free energy profile along the order parameter. The diffusion properties of the replicas can be used to asses the quality of the order parameter as a reaction coordinate.

In principle, one can easily parallelize RETIS by running each replica on a different node, and occasionally exchange paths during a swap move. A potential drawback is the fact that this is not optimal, as one has to wait until a shooting move has completely finished for all replicas before a swap move can be initiated. Because the paths are of different lengths, this means that most nodes will be waiting until the last replica has finished. This does not occur in regular TIS, where independent Markov chains are constructed. A simple solution might be to use the waiting time, for another simulation. This is rather unsatisfactory, but a better solution seems not so straightforward.

The RETIS method can be extended in several ways. First of all, different interfaces/replicas can be used for different channels. This doubles the number of interfaces, but removes the sampling problem of the asymmetric barrier, as both channels will now be equally well sampled. A potential problem is that one has to be able to distinguish in which channel the current path is. Besides, this will not work in case there are many different channels to sample.

Another possibility might be to treat the AA and AB paths independently from the BA and BB paths. This requires two sets of replicas where the indicator function restrict the pathways to begin either in A or in B. The two replica sets can exchange in the usually way among themselves, and, in addition, between the sets for AB paths only, as only these paths belong to both sets. This will give a better sampling of AA pathways on the downhill part of the barrier, where usually the BB paths have taken over, and of BB pathways on the uphill part of the barrier where the AA paths normally dominates.

ACKNOWLEDGMENTS

The author thanks Jutta Rogal for a critical reading of this manuscript.

APPENDIX: PATH SAMPLING FRAMEWORK

In this appendix, all path sampling methods are presented in one single framework. In Sec. A1 describes the flexible path sampling, followed by a recapitulation of TIS in terms of the new notation in Sec. A2. In Sec. A3 the possibility of biasing the shooting point toward the interface is explained. The replica exchange is introduced in Sec. A4.

1. Flexible path sampling

The probability of finding a certain trajectory $\mathbf{x}(L)$ is given by[8]

$$\mathcal{P}[\mathbf{x}(L)] = \rho(x_0)\prod_{i=0}^{L-1} p(x_i \to x_{i+1})/Z, \tag{A1}$$

where $\rho(x)$ denotes the steady state distribution, e.g., the canonical distribution, and $p(x \to y)$ represents the Markovian probability to go from a state x to y within one time

interval.[24] Z is normalization factor that is akin to a partition function and is given by

$$Z \equiv \int \mathcal{D}\mathbf{x}\rho(x_0)\prod_{i=0}^{L-1} p(x_i \to x_{i+1}), \tag{A2}$$

where the integration runs over all possible paths of all lengths.

The normalized path distribution given in Eq. (A1) can be sampled efficiently with importance sampling, in the form of the shooting algorithm.[8] This procedure selects a random shooting point x_j from an existing path, creates a new path by changing x_j, and shooting a new trajectory using the underlying dynamics, followed by accepting or rejecting according to a Metropolis acceptance criterion based on detailed balance.[20] In fact, it is easy to show that by assuming microscopic reversibility, a symmetric momenta generation, and an equal stationary and initial distributions the acceptance rule for the flexible path length shooting becomes rather simple

$$P_{\mathrm{acc}}[\mathbf{x}^{(o)} \to \mathbf{x}^{(n)}] = \min\left[1, \frac{L^{(o)}+1}{L^{(n)}+1}\frac{\rho(x_{sp}^{(n)})}{\rho(x_{sp'}^{(o)})}\right]. \tag{A3}$$

Here, the superscript o and n refer to the old and new paths, respectively. The factor involving length L appears into the acceptance, when the path length is allowed to change along the path sampling, because the *a priori* selection probability to choose a slice on a path is now not symmetric, but equals $1/(L+1)$. For fixed path length this factor is always unity. Note that the shooting point index sp' might be different from sp due to a different path length. This simple path sampling scheme, akin to hybrid molecular dynamics, will not be very efficient for unconstrained paths. The main advantage of transition path sampling arises from constraining the path to begin in a predefined initial region of phase space A, and end in another, final region B.

In the case of rare events one is not interested in sampling a stable state, but the barriers themselves. Therefore, it seems natural to only consider the parts of the paths connecting A and B that are *outside* of A and B, i.e., on the barrier. This naturally requires a flexible path length L as the time that is spent on the barrier can fluctuate.

A path sampling of rare events only should sample paths that lead over the barrier. This can be achieved by putting a constraint in the path distribution of Eq. (A1), such that only paths that connect A to B contribute to the distribution.

$$\mathcal{P}_{AB}[\mathbf{x}(L)] = h[\mathbf{x}(L)]\rho(x_0)\prod_{i=0}^{L-1} p(x_i \to x_{i+1})/Z_{AB}, \tag{A4}$$

with again Z_{AB} a normalizing factor.

$$Z_{AB} \equiv \int \mathcal{D}\mathbf{x}(L)h[\mathbf{x}(L)]\rho(x_0)\prod_{i=0}^{L-1} p(x_i \to x_{i+1}), \tag{A5}$$

where again the path integral runs over all paths of all lengths. The indicator function $h[\mathbf{x}(L)]$ is defined as

$$h[\mathbf{x}(L)] = \begin{cases} 1 & \text{if } x_0 \in A \wedge x_L \in B \wedge \\ & x_i \notin (A \cup B) \quad \text{for} \quad 0 < i < L \\ 0 & \text{otherwise}, \end{cases} \tag{A6}$$

such that the sampling this distribution only selects paths that just leave A, and just enter B. The Metropolis acceptance rule that allows the sampling of this distribution is

$$P_{\mathrm{acc}}[\mathbf{x}^{(o)} \to \mathbf{x}^{(n)}] = h[\mathbf{x}^{(n)}(L^{(n)})]\min\left[1, \frac{L^{(o)}+1}{L^{(n)}+1}\frac{\rho(x_{sp}^{(n)})}{\rho(x_{sp'}^{(o)})}\right], \tag{A7}$$

where $x_{sp'}$ and x_{sp} are the shooting points of the old and new paths, respectively (in most cases only differing in momenta). Note that in this notation the time index is renumbered such that the one time slice in state A has index zero. Note also that the indicator function of the old path does not appear in Eq. (A7), as it is by definition unity, because the old path belongs to the path ensemble. This flexible path procedure is a more efficient path sampling method than previous incarnations of the shooting algorithm because the path is never longer than strictly necessary.

As elaborated in Ref. 20 proper sampling of the transition path ensemble puts some restrictions on the stable state definition for A and B. A minor subtlety with the flexible path length approach is that the stable state definition should be slightly stricter than in the case of the fixed length shooting, because the algorithm assumes that once a path reaches a stable state it is truly committed to that state and will not recross the barrier for a time on the order of the reaction time.[10]

When stochastic dynamics is used one does not have to alter the momenta or positions at the shooting point because the stochastic nature of the dynamics will cause the trajectory to diverge from the old one.[20] In that case the acceptance rule changes into

$$P_{\mathrm{acc}}[\mathbf{x}^{(o)} \to \mathbf{x}^{(n)}] = h[\mathbf{x}^{(n)}(L^{(n)})]\min\left[1, \frac{L^{(o)}+1}{L^{(n)}+1}\right]. \tag{A8}$$

2. Transition interface sampling

Transition interface sampling focuses on the evaluation of Eq. (1). The flux factor ϕ_{01} can be computed directly in a straightforward dynamical simulation, by counting each effective positive crossing, i.e., the first crossing of interface λ_1 after having crossed λ_0. The second factor, the product of the crossing probabilities $P(\lambda_{i+1}|\lambda_i)$ is computed in a series of path sampling simulations. Depending on the number of interfaces and the interface spacing with respect to the height of the barrier, the interface crossing probabilities are within the range of 0.05–0.5. This means that a trajectory crossing interface λ_i now has a reasonable chance to reach the next interface λ_{i+1}. Each of the $P(\lambda_{i+1}|\lambda_i)$ crossing probabilities can be computed by performing a path sampling simulation that constrains the path to start in A, cross the interface λ_i, and end at λ_{i+1} or go back to A. Defining adjacent phase

space regions separated by interface λ_i as $\Lambda_i^+=\{x:\lambda(x)>\lambda_i\}$ and $\Lambda_i^-=\{x:\lambda(x)<\lambda_i\}$ the indicator function for this path ensemble becomes

$$\hat{h}_i[\mathbf{x}(L)]=\begin{cases}1 & \text{if } x_0\in A\wedge x_L\in(A\cup\Lambda_{i+1}^+)\wedge \\ & \forall\{j|0<j<L\}:x_j\notin(A\cup\Lambda_{i+1}^+)\wedge \\ & \exists\{j|0<j<L\}:x_j\in\Lambda_i^+ \\ 0 & \text{otherwise.}\end{cases} \tag{A9}$$

Note that this indicator definition uses a different notation than the time definition of the original TIS paper, in order to make the connection to the TPS path ensemble definition. However, it is formally equivalent to the expression used in the Appendix of Ref. 17. Note also that $A=\Lambda_0^-$ and $B=\Lambda_n^+$. This indicator function assigns only weights to paths that belong to the TIS ensemble

$$\mathcal{P}_{A\Lambda_i}[\mathbf{x}(L)]=\hat{h}_i[\mathbf{x}(L)]\rho(x_0)\prod_{j=0}^{L-1}p(x_j\to x_{j+1})/Z_{A\Lambda_i}, \tag{A10}$$

where the normalizing factor $Z_{A\Lambda_i}$ is again defined by $\int\mathcal{D}[\mathbf{x}]\mathcal{P}_{A\Lambda_i}[\mathbf{x}(L)]=1$. This distribution can be sampled with the same shooting algorithm as transition path sampling. The Metropolis acceptance rule thus becomes

$$P_{\mathrm{acc}}[\mathbf{x}^{(o)}\to\mathbf{x}^{(n)}]=\hat{h}[\mathbf{x}^{(n)}(L^{(n)})]\min\left[1,\frac{L^{(o)}+1}{L^{(n)}+1}\frac{\rho(x_{sp}^{(n)})}{\rho(x_{sp'}^{(o)})}\right], \tag{A11}$$

and for stochastic dynamics simplifies to

$$P_{\mathrm{acc}}[\mathbf{x}^{(o)}\to\mathbf{x}^{(n)}]=\hat{h}[\mathbf{x}^{(n)}(L^{(n)})]\min\left[1,\frac{L^{(o)}+1}{L^{(n)}+1}\right]. \tag{A12}$$

The algorithm for TIS sampling is given in detail in Ref. 10.

Based on the TIS ensemble of interface i the crossing probability $P(\lambda|\lambda_i)$ can be computed for each value of λ for the interval $\lambda_i<\lambda<\lambda_{i+1}$ from the histogram

$$P(\lambda|\lambda_i)=\langle\theta(\lambda_{\max}(\mathbf{x}(L))-\lambda)\rangle_{A\Lambda_i}, \tag{A13}$$

with $\lambda_{\max}(\mathbf{x})$ the maximum value of λ reached for each trajectory $\mathbf{x}$ in the path ensemble $A\Lambda_i$, and $\theta(x)$ is the Heaviside step function. The subscripted brackets denote the average

$$\langle\mathcal{O}(\mathbf{x}(L))\rangle_{A\Lambda_i}\equiv\int\mathcal{D}[\mathbf{x}]\mathcal{P}_{A\Lambda_i}[\mathbf{x}(L)]\mathcal{O}(\mathbf{x}(L)), \tag{A14}$$

where $\mathcal{O}$ denotes an arbitrary (path) observable. In fact, it is not necessary to limit the trajectories to the next interface λ_{i+1}. If instead the paths are allowed to go all the way to interface λ_B the TIS path distribution changes into

$$\mathcal{P}_{A\Lambda_i}[\mathbf{x}(L)]=\tilde{h}_i[\mathbf{x}(L)]\rho(x_0)\prod_{j=0}^{L-1}p(x_j\to x_{(j+1)})/Z_{A\Lambda_i}, \tag{A15}$$

with a new indicator function

$$\tilde{h}_i[\mathbf{x};L]=\begin{cases}1 & \text{if } x_0\in A\wedge x_L\in(A\cup B)\wedge \\ & \forall\{j|0<j<L\}:x_j\notin(A\cup B)\wedge \\ & \exists\{j|1<j<L\}:x_j\in\Lambda_i^+ \\ 0 & \text{otherwise,}\end{cases} \tag{A16}$$

in which the Λ_{i+1}^+ region of Eq. (A9) has been replaced by B. The crossing probability histograms in Eq. (A13) only differs from each other by a multiplicative factor. Therefore, all interface histograms can be joined together using the WHAM.[21]

In practice, one starts TIS with a full TPS simulation. From this ensemble one introduces an interface close to B which is then equilibrated. This is repeated for interface closer to A. During the sampling one should check if there is sufficient overlap of the histograms. If not, then a new interface can always be introduced.

The TIS methods can be equally defined for the reverse process $B\to A$, by reversing the labels B and A, and reversing the order of interfaces. As the RETIS explicitly makes use of the reverse ensemble, this will be explained in detail in Sec. IV.

3. Biasing the shooting point

Another way of improving efficiency is to bias the shooting point toward the interface. When the barrier is rather steep, shooting from near the stable state is not very likely to succeed. A shot from near the interface is much more likely to be accepted. Introducing a biasing function that selects shooting points around the interface can enhance the sampling. The shooting point selection probability for a time slice j becomes

$$p_{\mathrm{sel}}(j,\mathbf{x})=\frac{f(\lambda(x_j))}{\sum_{i=0}^{L}f(\lambda(x_{i\Delta t}))} \tag{A17}$$

in which case the acceptance criterion becomes [using the indicator function from Eq. (A9)]

$$P_{\mathrm{acc}}[\mathbf{x}^{(o)}\to\mathbf{x}^{(n)}]=\hat{h}[\mathbf{x}^{(n)}(L)]\min\left[1,\frac{\sum_{i=0}^{L^{(o)}}f(\lambda(x_i^{(o)}))}{\sum_{i=0}^{L^{(n)}}f(\lambda(x_i^{(n)}))}\right]. \tag{A18}$$

A possible biasing function might be Gaussian $f(\lambda)=\exp(-a(\lambda-\lambda_i)^2)$ centered around interface λ_i. The width of the Gaussian can be adjusted to optimize sampling (maximize decorrelation per CPU hour).

Alternatively, one can use an adaptive momenta change δp for the shooting point. A shooting point close to the barrier can sustain a much larger δp before the path will be rejected. If $\delta p(x_t)$ is a function of x_t the acceptance ratio will be given by Eq. (A11).

4. Replica exchange or path swapping

Although Sec. II suggests a sequential computation of the TIS ensembles, it is also possible to perform a computation of all interfaces simultaneously in parallel. As was proposed in Ref. 17 this allows for a replica exchange approach

also called path swapping. While most of the paths in the TIS ensemble i on the uphill side of the free energy barrier are returning quickly to A, resulting in a decreasing crossing probability as a function of λ, there is substantial probability that the next interface will be crossed as well. In fact, this is required to get an accurate estimate of the histogram $P(\lambda)$. When this happens, the path belonging to the λ_i interface is a valid member of the ensemble of λ_{i+1} interface, and vice versa. Therefore it is possible to exchange both paths between the ensembles without penalty. Exchanging paths between interface ensemble replicas can enhance ergodicity of the path ensemble substantially.

The total weight for all $n+1$ path ensembles together is

$$W = \prod_{i=0}^{n} \mathcal{P}_i[\mathbf{x}^{(i)}(L^{(i)})], \tag{A19}$$

where $\mathbf{x}^{(i)}$ and $L^{(i)}$ denotes, respectively, the current trajectory and its length of ensemble i (belonging to λ_i). The detailed balance rule for swapping replica i with j with symmetric generation probability is

$$P_{\mathrm{acc}}(i \leftrightarrow j) W^{(o)} = P_{\mathrm{acc}}(j \leftrightarrow i) W^{(n)}. \tag{A20}$$

The Metropolis acceptance rule is thus

$$\begin{aligned} P_{\mathrm{acc}}(i \leftrightarrow j) &= \min(1, W^{(n)}/W^{(o)}) \\ &= \min\left(1, \frac{\mathcal{P}_i[\mathbf{x}^{(j)}(L^{(j)})]\mathcal{P}_j[\mathbf{x}^{(i)}(L^{(i)})]}{\mathcal{P}_i[\mathbf{x}^{(i)}(L^{(i)})]\mathcal{P}_j[\mathbf{x}^{(j)}(L^{(j)})]}\right) \\ &= \min\left(1, \frac{\tilde{h}_i[\mathbf{x}^{(j)}(L^{(j)})]\tilde{h}_j[\mathbf{x}^{(i)}(L^{(i)})]}{\tilde{h}_i[\mathbf{x}^{(i)}(L^{(i)})]\tilde{h}_j[\mathbf{x}^{(j)(L^{(j)})}]}\right) \\ &= \min(1, \tilde{h}_i[\mathbf{x}^{(j)}(L^{(j)})]\tilde{h}_j[\mathbf{x}^{(i)}(L^{(i)})]) \\ &= \tilde{h}_i[\mathbf{x}^{(j)}(L^{(j)})]\tilde{h}_j[\mathbf{x}^{(i)}(L^{(i)})], \end{aligned} \tag{A21}$$

where the fourth line follows because the old paths belong always to their ensembles. In short, the swap is always accepted as long as path $\mathbf{x}^{(i)}$ belongs to the ensemble j and $\mathbf{x}^{(j)}$ belongs to i.

Paths in the first and last interface ensembles are rather short, and do only change slowly during sampling. To amend this, van Erp[18] proposed additional ensembles $\mathcal{P}^-$ and $\mathcal{P}^+$ for the first and last interface, respectively. For the first interface λ_1, a path in $\mathcal{P}^-$ starts with crossing λ_1 in the reversed direction and continues exploring the stable state A until the paths recrosses λ_1 in the positive direction again. This does allow for the paths to explore different parts of the λ_1 interface, thus tremendously increasing the exploration efficiency. Sampling this ensemble automatically leads to an estimate of the flux factor ϕ_{01} as this is simply equal to the inverse of the average sum of path lengths of the additional and the first interface ensemble $\phi_{01}=\langle \tau^- + \tau_1 \rangle^{-1}$. For the last interface a similar definition holds. The indicator function for the first additional ensemble $\mathcal{P}^-$ reads (remind that $\lambda_0=\lambda_A$)

$$\tilde{h}^-[\mathbf{x}(L)] = \begin{cases} 1 & \text{if } x_0 \in \Lambda_0^+ \wedge x_L \in \Lambda_0^+ \wedge \\ & \forall \{j | 0 < j < L\} : x_j \in A \\ 0 & \text{otherwise}, \end{cases} \tag{A22}$$

and for the additional ensemble $\mathcal{P}^+$ reads ($\lambda_n=\lambda_B$)

$$\tilde{h}^+[\mathbf{x}(L)] = \begin{cases} 1 & \text{if } x_0 \in \Lambda_n^- \wedge x_L \in \Lambda_n^- \wedge \\ & \forall \{j | 0 < j < L\} : x_j \in B \\ 0 & \text{otherwise}. \end{cases} \tag{A23}$$

van Erp shows in Ref. 18 that this approach is much more efficient than regular TIS.

Because in the replica exchange TIS all interface ensembles are sampled simultaneously the calculation of the reverse process B to A is also easily included. The indicator function that includes besides the AA and AB paths also the BA and BB paths is given in Eq. (5). The path probability for such combined ensemble is

$$\mathcal{P}_i[\mathbf{x}(L)] = \breve{h}_i[\mathbf{x}(L)]\rho(x_0)\prod_{j=0}^{L-1} p(x_j \to x_{j+1})/Z_i, \tag{A24}$$

where the normalizing factor Z_i is again defined by $\int \mathcal{D}[\mathbf{x}]\mathcal{P}_i[\mathbf{x}(L)]=1$. The indicator function $\breve{h}_i[\mathbf{x}(L)]$ selects paths that lead from A crossing the λ_i interface and reach A or B, or lead from B crossing the λ_i interface and reach A or B. The acceptance rule for stochastic dynamics is given as in Eq. (A12)

$$P_{\mathrm{acc}}[\mathbf{x}^{(o)} \to \mathbf{x}^{(n)}] = \breve{h}[\mathbf{x}^{(n)}(L^{(n)})]\min\left[1, \frac{L^{(o)}+1}{L^{(n)}+1}\right]. \tag{A25}$$

In analogy to Eq. (A21) the replica exchange swap acceptance for this ensemble is given by

$$P_{\mathrm{acc}}(i \leftrightarrow j) = \breve{h}_i[\mathbf{x}^{(j)}(L)]\breve{h}_j[\mathbf{x}^{(i)}(L)]. \tag{A26}$$

When the additional ensembles are included in the replica exchange, the swapping between the $\mathcal{P}^-$ and $\mathcal{P}_1$ is done by extending the path of the additional ensemble in the forward direction until it recrosses the interface λ_1, and extending the path in $\mathcal{P}_1$ ensemble in the backward direction until it recrosses the interface λ_0. If, such as in the current case, the $\lambda_A \equiv \lambda_0 = \lambda_1$, the old path is completely deleted, and only the two slices just before and after crossing the $\lambda_0(\lambda_1)$ interface remain. This swap move can always be accepted, as the paths in both the additional and the normal TIS ensemble always will cross their interface (see Ref. 18). The swap between $\mathcal{P}^+$ and $\mathcal{P}_{n-1}$ is done in a similar fashion.

[1] G. M. Torrie and J. P. Valleau, Chem. Phys. Lett. **28**, 578 (1974).
[2] E. A. Carter, G. Ciccotti, J. T. Hynes, and R. Kapral, Chem. Phys. Lett. **156**, 472 (1989).
[3] A. Laio and M. Parrinello, Proc. Natl. Acad. Sci. U.S.A. **99**, 12562 (2002).
[4] H. Grubmüller, Phys. Rev. E **52**, 2893 (1995).
[5] A. F. Voter, J. Chem. Phys. **106**, 4665 (1997).
[6] C. H. Bennett, in *Algorithms for Chemical Computations*, ACS Symposium Series No. 46, edited by R. Christofferson (American Chemical Society, Washington, DC, 1977).
[7] D. Chandler, J. Chem. Phys. **68**, 2959 (1978).
[8] C. Dellago, P. G. Bolhuis, F. S. Csajka, and D. Chandler, J. Chem. Phys. **108**, 1964 (1998).
[9] P. G. Bolhuis, D. Chandler, C. Dellago, and P. L. Geissler, Annu. Rev.

Phys. Chem. **53**, 291 (2002).
[10] T. S. van Erp, D. Moroni, and P. G. Bolhuis, J. Chem. Phys. **118**, 7762 (2003).
[11] D. Moroni, P. G. Bolhuis, and T. S. van Erp, J. Chem. Phys. **120**, 4055 (2004).
[12] A. K. Faradjian and R. Elber, J. Chem. Phys. **120**, 10880 (2004).
[13] D. Moroni, T. S. van Erp, and P. G. Bolhuis, Phys. Rev. E **71**, 056709 (2005).
[14] R. J. Allen, D. Frenkel, and P. R. ten Wolde, J. Chem. Phys. **124**, 024102 (2006a).
[15] R. J. Allen, D. Frenkel, and P. R. ten Wolde, J. Chem. Phys. **124**, 194111 (2006b).
[16] C. Valeriani, R. J. Allen, M. J. Morelli, D. Frenkel, and P. R. ten Wolde, J. Chem. Phys. **127**, 114109 (2007).
[17] T. S. van Erp and P. G. Bolhuis, J. Comput. Phys. **205**, 157 (2005).
[18] T. S. van Erp, Phys. Rev. Lett. **98**, 268301 (2007).
[19] T. J. H. Vlugt and B. Smit, PhysChemComm **2**, 1 (2001).
[20] C. Dellago, P. G. Bolhuis, and P. L. Geissler, Adv. Chem. Phys. **123**, 1 (2002).
[21] A. M. Ferrenberg and R. H. Swendsen, Phys. Rev. Lett. **63**, 1195 (1989).
[22] Note that one can use any interface for the flux calculation, as long as one uses the same interface for the conditional crossing probability.
[23] While I focus on two routes only, the RETIS method can sample as many routes as one can effort.
[24] These Markovian probability distributions depend on the dynamics. For instance, they are delta functions for Hamiltonian dynamics. For the Langevin dynamics employed in this paper they are given by bivariate Gaussian expressions (Ref. 8).